Tribology 2024 Intl. Conference

April 17 to 19, 2024, Vienna, Austria

Conference Proceedings

DOI:

https://doi.org/10.26799/cp-tribology-2024

Proceedings of the Tribology 2024 International Conference
Vienna, Austria – April 17 – 19, 2024
DOI: https://doi.org/10.26799/cp-tribology-2024

$BaTiO_3$ /UHMWPE Composites for Enhanced Performance in Load-Bearing Biomedical Implants

Darshana Havaldar [1], Zdeněk Starý[2], Jan Walter[1], Ladislav Cvrček[1], Roman Gabor[3], Zdeňka Jeníková[1], Kiran Pawar[4]
[1]Department of Materials Engineering, Faculty of Mechanical Engineering, Czech Technical University in Prague, Karlovo náměstí 293/13, 120 00 Prague 2, Czechia, darshana.havaldar@fs.cvut.cz
[2] Department of Polymer Processing, Institute of Macromolecular Chemistry, Czech Academy of Sciences, Heyrovského nám. 1888, Břevnov, 162 00 Praha 6, Czechia, stary@imc.cas.cz
[3] Nanotechnology Centre, CEET, VSB – Technical University of Ostrava, listopadu 2172/15, 708 00 Ostrava 8, Czechia, roman.gabor@vsb.cz
[4] School of Nanoscience and Biotechnology, Shivaji University, Vidya Nagar, Kolhapur, Maharashtra 416004, India

Abstract

The pursuit of advanced biomaterials for load-bearing applications in biomedical implants has incited the development of polymer composites tailored for optimal mechanical properties, wear resistance, and biocompatibility. This research emphasises developing and characterizing polymer composites based on Ultra-High Molecular Weight Polyethylene (UHMWPE) reinforced with Barium Titanate ($BaTiO_3$) nanoparticles. To assess the suitability of the composite for load-bearing biomedical implants, five distinct combinations of UHMWPE and $BaTiO_3$ were manufactured by a compression molding process and tested with mechanical, surface, and tribological studies. The mechanical behaviour of the $BaTiO_3$/UHMWPE composites indicates enhancements in tensile strength, flexural strength, and impact resistance, crucial to ensuring the mechanical integrity required in load-bearing applications. The surface wettability of the composites was analysed with the contact angle measurements, providing insight into their interaction with biological fluids. Hardness testing was employed to assess the resistance of the materials to deformation and wear. Tribological testing, using a pin-on-disc tribometer, explored friction and wear behaviour, essential for predicting their performance within the human body under load-bearing conditions. The composites were characterized by light microscopy, Scanning Electron Microscopy (SEM), and Differential Scanning Calorimetry (DSC). The study reveals the potential of $BaTiO_3$/UHMWPE composites as biomedical implant materials due to their mechanical strength, hardness, and tribological properties. These composites are suitable for applications that require low wear and high structural integrity of the material. Their biocompatibility and therefore applicability for biomedical applications must be further evaluated.

Keywords: UHMWPE, $BaTiO_3$, polymer composites, biomedical implants, load-bearing, mechanical properties, biocompatibility, tribological performance

1. Introduction

Polymer matrices with incorporated nanofillers have emerged as a promising class of materials over the past few decades, often addressing crucial needs in biomedical engineering including structural integrity, controlled drug release, minimized wear, etc. due to their innate mechanical strength, biocompatibility, and ability to tailor functionalities. However, the introduction of novel composite materials, fabrication methods, and detailed insight into their interaction with biological entities have hastened the research [1], [2], [3].

On the other hand, one must take care of considerable challenges that could restrict use such as ensuring long-term stability, interfacial interactions, and attaining uniform dispersion of nanosized fillers while developing and implementing these advanced materials [4].

This research work intends to study the competency of polymer composites that are mainly focused on load-bearing implant applications. Hence, accordingly, the combination of Ultra High Molecular Weight Polyethylene (UHMWPE) as a matrix (acknowledged for biocompatibility and excellent wear resistance) and Barium Titanate ($BaTiO_3$) as a filler (a ferroelectric ceramic with piezoelectric

DOI: https://doi.org/10.26799/cp-tribology-2024

properties) has been chosen and fabricated meticulously by compression molding [5], [6]. As a result, the fabricated nanocomposites are expected to modify and reflect the unified properties inherited by each of the materials notably, mechanical durability, biocompatibility, and stimulus-based response. The following text addresses the fabrication, testing, characterisation, and potential applicability of composites.

2. Materials and methods

The UHMWPE (powder grade GUR 4120) was used as a matrix, and $BaTiO_3$ as a nanofiller. Isopropanol was employed as a dispersant to form colloidal formations of materials. Polymer composites of $BaTiO_3$/UHMWPE were fabricated at five different weight percentages of filler from 0 to 10wt%. The sample formulation was carried out using an ultrasonication bath by dispersing specific amounts of UHMWPE and BaTiO3 in isopropanol. The resulting mixture was stirred mechanically in the second place, and then the mixture was dried in an oven to remove the moisture entirely. The formulated powder was molded in sheets using a hot compression molding process. The synthesized composites are labelled C1, C2, C3, C4, and C5. The level of filler in the composite increases progressively from C1 (0wt%) to C5 (10wt%).

Composite characterization

To assess the strength and adequacy of the composites for load-bearing applications, mechanical tests were performed. Both tensile tests and three-point flexural tests were executed on a universal testing machine. The Charpy impact test was undertaken at room temperature to analyse the impact strength of composites using an impact tester. The Vickers hardness tester rendered measurements of the hardness of the materials. Contact angle measurement helps to assess the ability of composites to interact with biological fluids and promote tissue integration. Hence, to quantify the interaction of the composite surface with liquid, a droplet of distilled water was released on the composite surface, and the image of the liquid-droplet interface was recorded by a light digital microscope.

Tribological testing was conducted using the pin-on-disc tribometer. The tests were carried out with an Al_2O_3 counter body, a 6 mm diameter, on air and in a solution of phosphate buffered saline (PBS) to simulate the environment of the human body. The wear of the counter body surface and the wear track on the planar sample were analysed using a light digital microscope after the test. For all combinations, the specific wear rate (k) was calculated from the equation:

$$k = \frac{V}{F\,s} \tag{1}$$

where V is the wear volume, F is the normal load, and s is the sliding distance. The wear volume was obtained by multiplying the area of the wear track cross-section, measured by the coherence scanning interferometer, by the circumference of the wear track. A differential scanning colorimeter was availed to parse the melting and crystallization temperature as well as the melting enthalpy of samples. The degree of crystallinity (Xc) of the nanocomposites was calculated by:

$$\mathrm{Xc} = \frac{\Delta Hm}{(1-\omega)\Delta H_m^0} \cdot 100\% \tag{2}$$

where ΔH_m is the measured heat of fusion, ΔH_m^0 is the heat of fusion of 100% crystalline UHMWPE (291 J g^{-1}), and w is the weight fraction of $BaTiO_3$ in the polymer matrix.

3. Results and discussion

The results of the tensile test (tensile strength, yield strength, and Young's modulus) and flexural strength were recorded and plotted in Figure 1. It emerged that the incorporation of $BaTiO_3$ has influenced the modulus positively; however, tensile strength, yield strength, and flexural strength initially stepped up with the addition of filler followed by a slight diminution. Yet the values are still higher than those of neat UHMWPE. Composites displayed a nonlinear relation between filler concentrations and impact strength (Fig. 2a). Although the impact strength of C2 and C5 indicated a decline in strength in comparison to neat UHMWPE (C1), the C3 and C4 samples presented optimum impact resistance, conceivably due to better distribution and reinforcement in these formulations. Figures 2b and 2c reveal

DOI: https://doi.org/10.26799/cp-tribology-2024

how filler concentration alters surface wettability and indentation resistance. The contact angle shifted to further hydrophilic as the filler reached a maximum; concurrently, Vickers hardness unveiled a slight rise across the similar filler range.

During dry sliding of tribological testing, all samples' friction coefficient was stable in the range of 0.1-0.13, except C3, where COF was somewhat lower than 0.1. The specific wear rate of all composites tested on air was lower than that of pure UHMWPE, especially for the C3, the wear was less than half that of UHMWPE. During the tests in phosphate-buffered saline, C2, C3, and C5 composites lodged a lower coefficient of friction falling within the range of 0.02-0.06, than the neat polymer sample.

The DSC analysis indicates that the presence of BaTiO3 slightly influences the crystallinity of the composite, with the C5 composite showing the highest crystallinity among the tested samples (Fig. 2d). SEM micrograph of the composite film was captured to perceive the morphology coupled with the distribution of filler within the matrix, as shown in Fig. 3b.

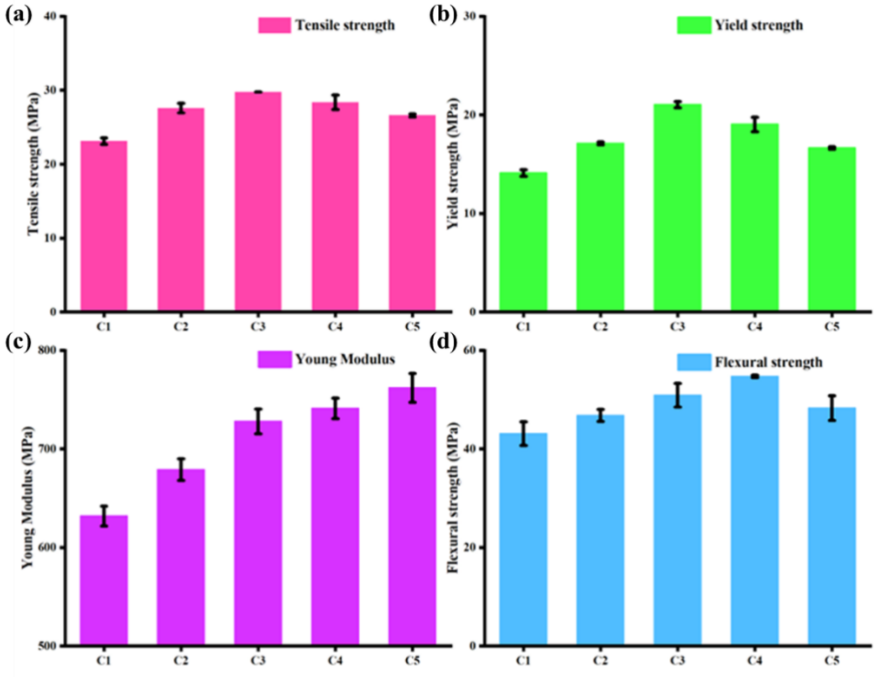

Fig. 1: The graphs of (a) Tensile strength, (b) Yield strength, (c) Young's modulus, and (d) Flexural strength of C1, C2, C3, C4, and C5 composites.

DOI: https://doi.org/10.26799/cp-tribology-2024

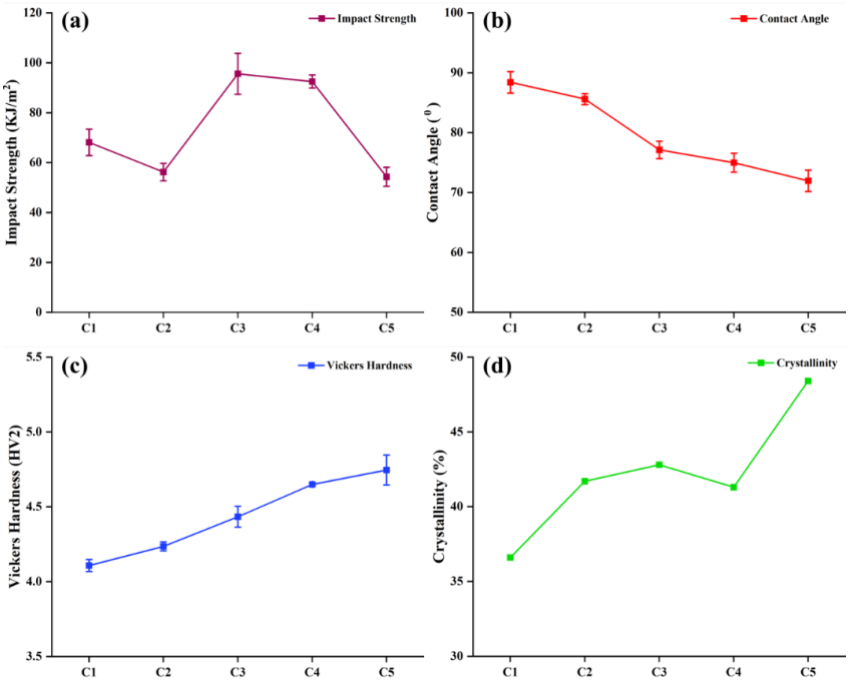

Fig 2: The graphs of (a) Impact strength, (b)Contact angle, (c) Vickers Hardness, (d) Crystallinity of C1, C2, C3, C4, and C5 composites.

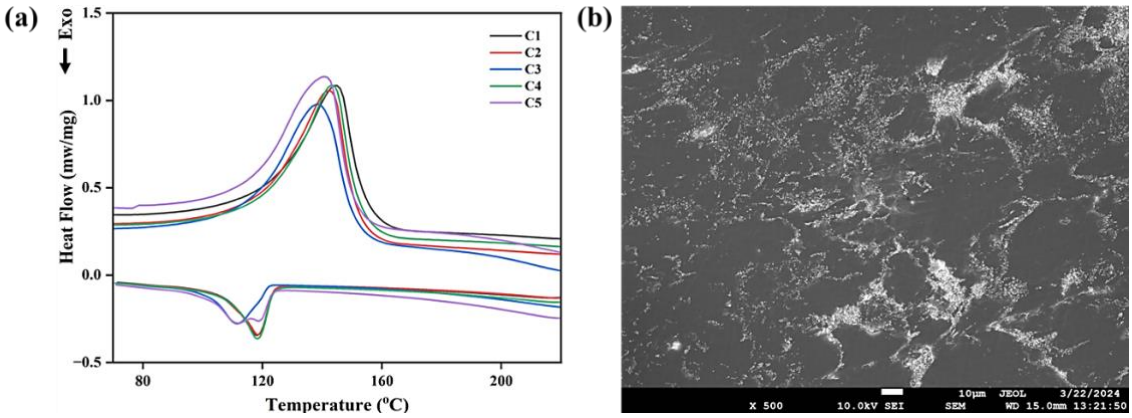

Fig. 3: (a) DSC curves and (b) SEM image of the composites.

4. Conclusion

The study discloses the potential use of $BaTiO_3$/UHMWPE nanocomposites as biomedical implant material. Composites showcased improvements in mechanical strength, hardness, and tribological properties, which were well suited for applications with reduced wear applications, accompanied by a hydrophilic surface appropriate for interactions with biological fluids. However, their biocompatibility and therefore applicability for biomedical applications need to be further evaluated.

Acknowledgment

This work was supported by the Grant Agency of the Czech Technical University in Prague project No. SGS23/163/OHK2/3T/12 and as part of the project No. CZ.02.01.01/00/22_008/0004631, Materials and technologies for sustainable development within the Jan Amos Komensky Operational Program financed by the European Union and from the state budget of the Czech Republic.

References

1. M. Abbas, M. S. Alqahtani, and R. Alhifzi, "Recent Developments in Polymer Nanocomposites for Bone Regeneration," *International Journal of Molecular Sciences*, vol. 24, no. 4. Multidisciplinary Digital Publishing Institute (MDPI), Feb. 01, 2023.
2. N. Dalai and P. S. R. Sreekanth, "UHMWPE / nanodiamond nanocomposites for orthopaedic applications: A novel sandwich configuration based approach," *J Mech Behav Biomed Mater*, vol. 116, Apr. 2021.
3. A. Pokkalath, D. Nadar, P. Ravikumar, and S. P. Sawarkar, "Nanomaterials for orthopaedic implants and applications," *Handbook on Nanobiomaterials for Therapeutics and Diagnostic Applications*, pp. 229–270, Jan. 2021.
4. R. Pfaendner, "Nanocomposites: Industrial opportunity or challenge?," *Polym Degrad Stab*, vol. 95, no. 3, pp. 369–373, Mar. 2010.
5. E. Gomez-Barrena, J. A. Puertolas, L. Munuera, and Y. T. Konttinen, "Update on UHMWPE research: From the bench to the bedside," *Acta Orthopaedica*, vol. 79, no. 6. pp. 832–840, Dec. 01, 2008.
6. V. Buscaglia, M. T. Buscaglia, and G. Canu, "BaTiO3-based ceramics: Fundamentals, properties and applications," in *Encyclopedia of Materials: Technical Ceramics and Glasses*, vol. 3–3, Elsevier, 2021, pp. 311–344.

Proceedings of the Tribology 2024 International Conference
Vienna, Austria – April 17 – 19, 2024
DOI: https://doi.org/10.26799/cp-tribology-2024

Measuring Bearing Loads – Practical Implementation of Impedance Measurement in a Machine Tool Spindle

S. Puchtler [1], M. Fett [1], G. Martin [2], E. Kirchner [1]
[1] Institute for Product Development and Machine Elements, Technical University of Darmstadt, Otto-Berndt-Str. 2, 64287 Darmstadt, Germany, office@pmd.tu-darmstadt.de
[2] HCP Sense GmbH, Robert-Bosch-Str. 7, 64293 Darmstadt, Germany, martin@hcp-sense.com

Abstract

Tribological contacts are at the heart of manifold mechanical processes. With Industry 4.0, the interest in information about process parameters increases consistently. Therefore, researchers strive to gain valuable information from as close to the process as possible. A promising approach to measure in-situ right in the tribological contact is electrical impedance. In the area of ball bearings, models have been developed based on test rig results. In this work, findings were transferred to the practical implementation in a machine tool spindle for the first time. First, preliminary tests were carried out on a rolling bearing test bench. On this test rig, interference factors and interactions could be minimized and operating parameters such as speed, axial and radial loads could be reproducibly set and varied. Based on these findings, tests were carried out on an electrically adapted sensor spindle design by Christ Industries. Although the step from the individual bearing to the sensor spindle has greatly increased the system complexity and thus the potential for interference, measured values showed good quality. Subsequently, the sensor spindle was installed and integrated into the whole system of a machine tool by Datron. A force measuring platform was used to measure the forces that occur during the chipping process. By comparing these forces with the measured impedance, it was possible to confirm the usability of the bearings as sensors. Axial loads, as they occur during drilling processes, are clearly recognizable in the impedance signal. It was possible to derive an almost linear relationship between the axial load and the bearing capacitance. Taking the influences of temperature and speed into account, an evaluation model was developed, that allows the interpretation of the measured impedance signal and the derivation of the axial forces acting on the spindle.

Keywords: ball bearings, machine tool spindle, in-situ measurement, bearing impedance, condition monitoring, EHL-contact, lubrication film thickness

1. Introduction

Manufacturers of machine tools often have no insight into how their customers use the machine tools in practice, for example whether recommendations regarding load or operating conditions are followed. This can lead to challenges, especially when it comes to service and warranty claims. Although measuring systems exist to monitor the forces acting during operation, these are very expensive and difficult to integrate into the overall system. In order to address this challenge, a project was carried out to adapt the tool spindle so that the impedance of the spindle bearings can be measured and used as a sensor during operation.

The electric impedance of a bearing is majorly influenced by the ball-raceway contacts. In hydrodynamic lubrication, e.g., the typically high-resistive lubricant acts as a dielectric, forming a capacitor which influences the electrical behavior. This in return can be utilized to monitor run-in [1], lubrication [2] and load [3] of a bearing. Therefore, impedance models are continuously improved [3–5], delivering the theoretical background to the measuring principle used in this work.

Proceedings of the Tribology 2024 International Conference
Vienna, Austria – April 17 – 19, 2024
DOI: https://doi.org/10.26799/cp-tribology-2024

2. Materials and Methods

In this work, the experimental test results will be qualitatively compared to calculation results retrieved by a model described in [3]. The necessary parameters were retrieved from the bearing's and lubricant's data sheet and completed by values from comparable bearings and oils. As the permittivity of the base oil was unknown, it was set to $\varepsilon_{\mathrm{Oil}} = 6{,}2$ for a best fit with the experimental results.

The test rig used allows radial and axial loading of a test bearing on a shaft supported by three hybrid support bearings. Insulated bearing seats and a slip ring allow a defined current path through the bearing. Further details of the test rig can be found in [3] and [4].

The sensor-integrated motor spindle utilizes the effect that the electrical impedance of the bearings depends on the mechanical load on them. In order to measure this impedance with the sensor-integrated motor spindle, the outer ring of the bearing must be contacted. A slip ring contact enables current or voltage to be transmitted to the inner ring. The existing spindle design was adapted to accommodate contact pins as well as cables and connectors for contacting the outer rings of the rolling bearing and the shaft. The temperature sensors required for impedance measurement were also integrated. The bearing seats were also insulated from the rest of the system to prevent interference. As the rolling elements must be conductive, it is not possible to use ceramic ones. Thus, steel bearings were used instead of hybrid bearings.

3. Results and Discussion

Fig. 1a shows calculation results of the bearing und lubricant used in the spindle. The gray box shows the estimate typical operating range of the bearing. It can be seen, that the sensitivity of the capacitance to the radial load is significantly lower than to the axial load. The reason for this can be seen in **Fig. 1**b, where the series capacitance of inner and outer contact for each rolling element is displayed in a polar plot. At pure axial load (load angle $\beta = \arctan(F_\mathrm{a}/F_\mathrm{r}) = 90°$) each rolling element contributes the same share to the total capacitance. If a radial load equal to the axial load is added ($\beta = 45°$), the rolling elements in direction of the radial load reach a higher capacitance. On the other hand, the opposite rolling elements are relieved, resulting in a lower capacitance. Therefore, the total capacitance stays almost constant in this operation range.

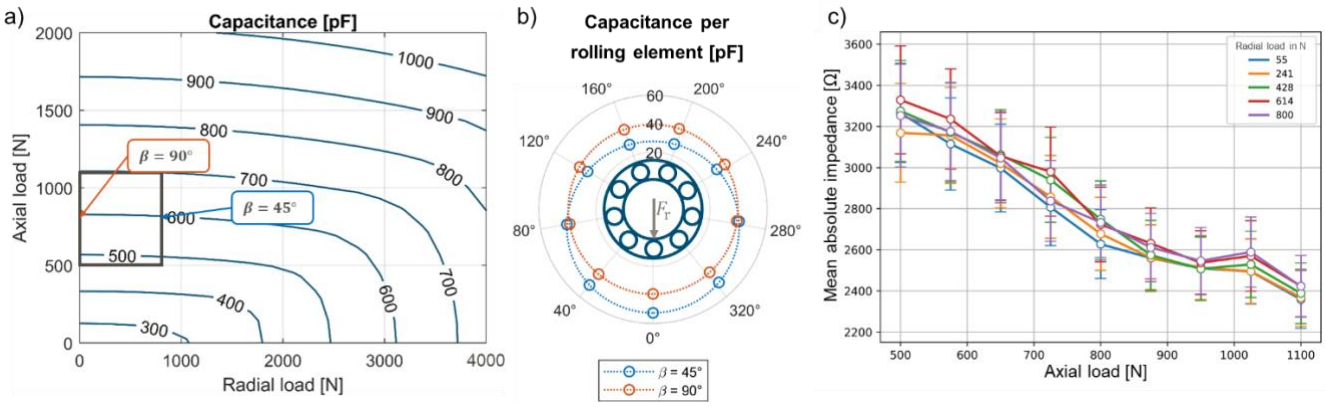

Fig. 1: a/b) Calculation results for a 6005 spindle bearing with PAO/E grease at speed $n = 6000$ rpm and temperature $T = 35°\mathrm{C}$. a) Total bearing capacitance in dependency of radial and axial load. The box indicates the typical operation range of the spindle bearing. b) Polar plot of the capacitance contributions of the individual rolling elements. Red: Pure axial load of $F_\mathrm{a} = 800$ N, blue: combined load of $F_\mathrm{r} = F_\mathrm{a} = 800$ N. c) Experimental results for the impedance at $f = 100$ kHz at different axial and radial loads and constant speed of $n = 6000$ rpm and average temperature of $T = 35°\mathrm{C}$.

The tests on the rolling bearing test bench provided insights into the physical relationships between axial and radial force, temperature, speed and impedance. The impedance measurement is carried out using the impedance analyzer MFIA by Zurich Instruments. A sensory utilizable correlation was observed between the axial force acting on the bearing and the measured impedance. As the axial force increases, the absolute value of the bearing impedance decreases. The acting radial force, on the other hand, has no traceable and therefore no sensory usable influence on the bearing impedance. The theoretical explanation for these observations is, as previously shown, that with an axial load on the bearing, all rolling elements are loaded equally, which has a comprehensible influence on the impedance. A radial load, on the other hand, increases the load on the rolling

DOI: https://doi.org/10.26799/cp-tribology-2024

elements within the load zone, but at the same time relieves the rolling elements on the opposite side of the bearing. This can result in the influences on the overall impedance of the bearing balancing each other out. Fig. 1c shows the course of the mean value of the bearing impedance over the axial load for different radial loads.

During the spindle tests, controlled speed ramp-ups were carried out without applying force. The speed was increased from 0 to 30,000 rpm over a period of 30 seconds. The analysis of the measured data in the frequency range using fast Fourier transformations (FFT) allows the data to be converted into waterfall diagrams. The respective speeds are plotted on the y-axis. The frequencies are plotted on the x-axis, while the color coding indicates the respective amplitudes. Bearing-characteristic, speed-dependent phenomena can be observed. In particular, the rollover frequencies of the inner ring, the outer ring and the rolling elements can be seen as a function of the speed. Furthermore, multiple of these phenomena can be recognized as well as a modulation of the phenomena with the inverter frequency of the electric drive of 8 kHz. **Fig. 2**a shows a waterfall diagram of the bearing's impedance. In **Fig. 2**b, the FFT at $n = 20{,}000$ rpm is shown.

In addition to the impedance measurement, vibration measurements were carried out using a Brüel & Kjær vibration measurement system. These are very similar to those of the impedance measurement and confirm their plausibility, cf. **Fig. 2**c. Unlike the vibration signal, no resonance frequencies in the form of vertical lines are visible in the impedance waterfall diagram.

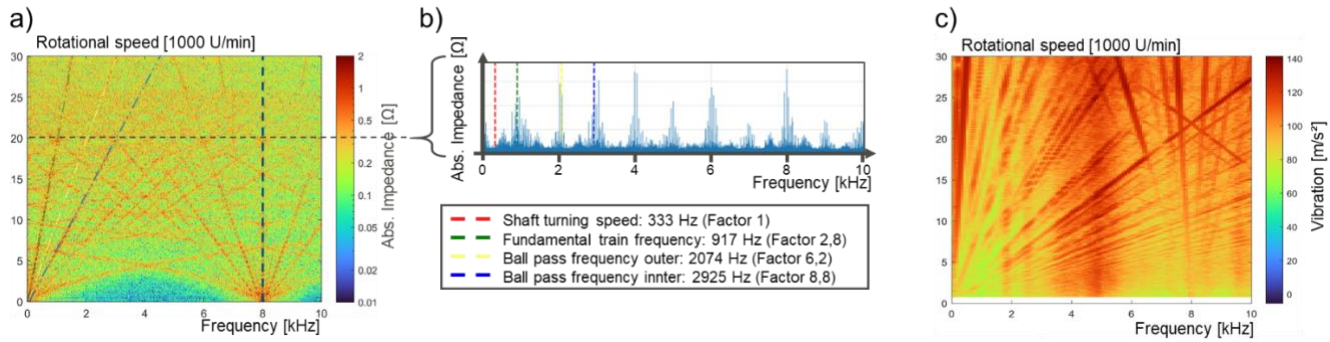

Fig. 2: Free running tests of the machine tool spindle during a run-up from $n = 0 \ldots 30{,}000$ rpm. a) Waterfall diagram of the impedance, b) FFT at $n = 20{,}000$ rpm and c) waterfall diagram of the vibration signal.

Finally, tests were then carried out on the entire machine tool with the spindle installed. In addition to the measurement systems of the spindle, the force measurement platform Dynamometer 9257B from Kistler was used to record forces in each spatial direction during drilling. In the machining area of the machine tool an aluminum cuboid was clamped onto the force measuring platform. This allowed the forces acting on the raw material and, in interaction with it, the forces acting on the spindle to be measured. **Fig. 3**a shows the bearing capacitance and axial load measurement over time. It can be seen that the capacitance follows the load measurement qualitatively. By plotting the load over the capacitance an almost linear relationship can be observed, **Fig. 3**b. The influencing variables of temperature and speed can be largely eliminated by scaling, **Fig. 3**c. The remaining pitch error can be partially explained by the different temperatures of the bearing at the time of measurement ranging from 20.5°C to 25.5°C.

4. Conclusion

In this work, the practical implementation of a sensory utilized ball bearing in a machine tool spindle was described. Tests on the test bench were in line with calculation results. In the investigated set of operating parameters, the axial load had a high influence on the impedance as the radial load in this range had an insignificant influence. Spindle run-ups showed a good visibility of bearing frequencies without any resonances visible unlike the corresponding vibration measurement. Drill tests showed an almost linear relationship between capacitance and load. By normalizing the capacitance before the drill process, some disturbance factors like temperature can be eliminated to a certain degree.

DOI: https://doi.org/10.26799/cp-tribology-2024

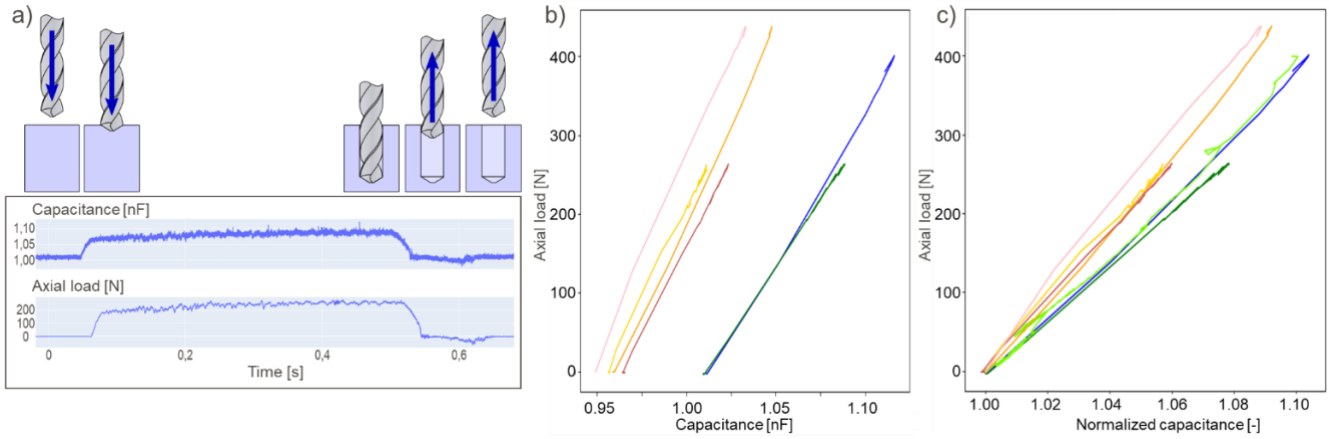

Fig. 3: Drilling tests of the assembled machine tool a) over time, b) axial load over capacitance and c) over the normalized capcitance at $n = 12{,}000$ and 30,000 rpm, diameter 3 mm, depth 15 mm, feed rate 2000 and 4000 mm / min.

Acknowledgements

The results were achieved as part of the project “ImpSpin”, funded by the state of Hesse (Germany) and the Distr@l programme, for which we would like to express our gratitude. We would also like to thank the project partners, namely the companies DATRON AG, CHRIST-Feinmechanik GmbH & Co. KG, optiMEAS Measurement and Automation Systems GmbH as well as the Institute for Production Management, Technology and Machine Tools (PTW) of the Technical University of Darmstadt.

References

1. S. Schnabel, P. Marklund, I. Minami, and R. Larsson, "Monitoring of Running-in of an EHL Contact Using Contact Impedance," *Tribol Lett*, vol. 63, no. 35, 2016, doi: 10.1007/s11249-016-0727-2.
2. T. Maruyama, M. Maeda, and K. Nakano, "Lubrication Condition Monitoring of Practical Ball Bearings by Electrical Impedance Method," *Tribology Online*, vol. 14, no. 5, pp. 327–338, 2019, doi: 10.2474/trol.14.327.
3. S. Puchtler, J. van der Kuip, and E. Kirchner, "Towards White-Box Modeling of Sensory-Utilized Rolling Bearings," in *10th ECCOMAS Thematic Conference on Smart Structures and Materials*, Patras, Greece, D. Saravanos and A. Benjeddou, Eds., 2023, pp. 1635–1645, doi: 10.7712/150123.9935.444456.
4. S. Puchtler, J. van der Kuip, and E. Kirchner, "Analyzing Ball Bearing Capacitance Using Single Steel Ball Bearings," *Tribol Lett*, vol. 71, no. 2, 2023, doi: 10.1007/s11249-023-01706-7.
5. A. Gonda, S. Paulus, S. Graf, O. Koch, S. Götz, and B. Sauer, "Basic experimental and numerical investigations to improve the modeling of the electrical capacitance of rolling bearings," *Tribology International*, vol. 193, p. 109354, 2024, doi: 10.1016/j.triboint.2024.109354.

Proceedings of the Tribology 2024 International Conference
Vienna, Austria – April 17 – 19, 2024
DOI: https://doi.org/10.26799/cp-tribology-2024

Abrasion of Polyester Sportswear Materials: The Impact of Yarn Parameters and Aging

G. Čubrić [1*], I. Salopek Čubrić[2], A. Petrov[1]
[1] University of Zagreb Faculty of Textile Technology, Department of Clothing Technology, Prilaz baruna Filipovića 28 a, Zagreb, Croatia
[2] University of Zagreb Faculty of Textile Technology, Department of Textile Design and Management, Prilaz baruna Filipovića 28 a, Zagreb, Croatia

Abstract

In the world of sports equipment, especially in the production of sportswear, the challenge of maintaining the durability of materials is becoming increasingly crucial to ensure performance and lasting quality. This scientific paper explores a set of materials intended for the production of football jerseys, all made of 100% polyester (both standard and recycled). The focus of the research is on the resistance of materials to abrasion. The resistance to abrasion was investigated for non-used materials, as well as for the materials that were aged. The aging of materials was in the form of the exposure to sunlight for 80 hours, simulating conditions during football games. The key phase of the research is centered on material abrasion before and after aging that is investigated using the AquaAbrasion tester. Through the simulation of 2500 and 5000 cycles of abrasion, the aim was to determine the durability of the materials and how their properties change due to use and aging. Related to it, additionally are observed the changes in the structure density, mass per unit area, and thickness. Special attention is given to recycled polyester material, exploring its sustainability and impact on quality compared to other materials. The results of this research provide valuable insights into the practical application of these materials in the production of sportswear and potential steps toward improving their durability and sustainability.

Keywords: abrasion, durability, yarn, sportswear, football, recycled, polyester, aging, sustainability

1. Introduction

In the world of the production of sportswear, the challenge of maintaining the durability of materials is becoming increasingly crucial in order to ensure optimal performance during use and lasting quality. The creation of fibers and yarns for the manufacture of upscale sportswear has advanced significantly in recent years, as has the ongoing exploration of novel ideas in the field of sportswear design. Comfort is unquestionably a key component of sportswear. One of the key factors in determining a garment's quality is its level of comfort. Ensuring sportsmen to have optimal comfort when donning gear is crucial, especially during actual competition. In order for water vapor to diffuse through the pores and into the surroundings when the body is moving, the textile used to make the clothing needs to have a high porosity. To maintain the best possible thermoregulation of the human body, sportswear also needs to have excellent ventilation, a high degree of moisture permeability, and thermal insulation in cold weather [1, 2]. Textile materials deteriorate with time and continuous use due to several factors, including material abrasion from contact with different surfaces and media. Rubbing fibers against one another or against a different material causes abrasion. The ability of a material to withstand surface abrasion brought on by frictional contact with another material is known as abrasion resistance. Poor abrasion resistance causes fibers to degrade and wear out more quickly. Abrasion shows signs of wear on the material [3, 4]. Many researchers have investigated how abrasion affects materials. These investigations have looked into the abrasion resistance of woven fabric [5], the effect of abrasion on synthetic textiles on the development of microplastic fibers [6], and the relationship between material aging and the abrasion resistance of knitted fabrics that have elastane added [7].

This scientific paper explores a set of materials intended for the production of football jerseys, all made of 100% polyester (both standard and recycled). The focus of the research is on the resistance of materials to abrasion.

DOI: https://doi.org/10.26799/cp-tribology-2024

2. Experiment

2.1. Materials

For the investigation presented in this paper, a set of materials intended for the production of football sportswear is used. All the materials are made of 100% polyester, either standard or recycled. As can be seen from the Table 1, besides the type of polyester used, the materials differ in mass per unit area.

Table 1 Overview of polymeric materials

Nr.	Polymeric material ID	Polymer type	Mass per unit area, g/m^2
1.	KM1	recycled	130
2.	KM2	standard	155
3.	KM3	standard	151
4.	KM4	standard	145

2.2. Materials aging

To simulate material aging, polymeric materials were exposed to defined outdoor conditions and care procedures that correspond to the conditions to which the sportswear of a professional football player is exposed. More specifically, the materials were exposed to direct sunlight, sweating with an artificial sweat solution sprayed onto the material surface and a standard washing procedure. The materials were exposed to direct sunlight in the morning (from 8:00 to 12:00) at an average air temperature of 25±2 °C, an average relative humidity of 66±5 % and an average wind speed of 4±2 m/s. The exposure lasted a total of 80 hours.

2.3. Testing Method

The AquAbrasion – Wet and Dry Abrasion Tester from James Heal, UK, is used to measure the abrasion of polymer materials (Fig. 1). The AquAbrasion is based on the Martindale device, but also uses a controlled pump system to inject liquid into the fabric samples to keep them wet for the duration of the test. The abrasion test was carried out according to the procedure described in the international standard ISO 12947-3:1998 [8]. Samples of polymeric materials (both non-aged and aged) were cut to a diameter of 38 ± 5 mm and prepared for the test. The standard wool fabric was used for the abrasion test. The round sample is clamped in the sample holder and subjected to a specific load, rubbing against the abrasion medium in a translatory motion according to the Lissajous figure. A standard pressure of 9 kPa was used. The method of mass loss of the test specimens was used to estimate the abrasion resistance of the polymeric materials. According to the method, each sample was weighed before the test and after a certain number of test cycles. For this experiment, the following number of abrasion cycles were defined: 2500 and 5000 cycles. The mass of the samples was determined using a KERN ALJ- 220 analytical balance with an accuracy of +/- 0.001 g.

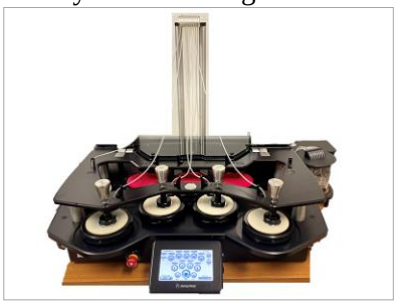

Fig. 1: The AquAbrasion – Wet and Dry Abrasion Tester

3. Results and Discussion

The abrasion results of the non-aged materials are shown in Figure 2. The materials were subjected to abrasion in 2500 and 5000 cycles. Sample KM1 made of recycled polyester, showed the lowest mass of all tested samples. The graph clearly shows that after 2500 abrasion cycles there is a slight increase in mass for all tested materials. This can be attributed to the infiltration of fine fibers into the material structure. These fibrous elements penetrated the material from the wool backing on the abrasion device, on which the samples were placed. This process can result in a temporary increase in the mass of the material. After 5000 abrasion cycles, the materials were exposed to an air flow to remove additional fibers from the material structure. This procedure has a potentially effective role in restoring the original structure of the material and removing the elements that contributed to the increase in mass after 2500 cycles. This process resulted in a significant reduction in mass

DOI: https://doi.org/10.26799/cp-tribology-2024

for all materials tested. Mass decrease after 5000 cycles for material KM1 is 1.80%, for KM2 0.92%, for KM3 1.35%, and for KM4 1.55%.

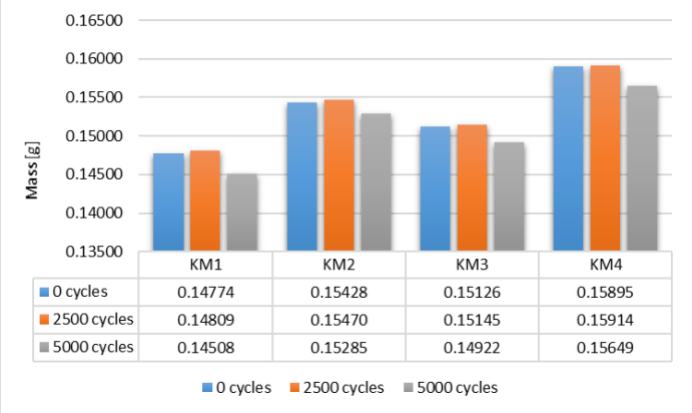

Fig. 2: Graphical presentation of measured masses after a different number of cycles for non-aged materials

Figure 3 gives an insight into the changes of mass of the aged materials after 2500 and 5000 abrasion cycles. As with the non-aged materials, the materials were blown after 5000 abrasion cycles to remove additional fibers that had penetrated the knit structure during abrasion on the wool backing. It is noticeable that the initial mass of materials KM1 and KM2 prior to abrasion is greater for aged materials compared to non-aged ones. This increase in mass can be related to the aging of the materials. Aging, particularly the 80-hour exposure to sunlight, may have led to changes in the structure of the material, including the possible absorption of moisture or other substances, resulting in increased mass. In comparison, the KM3 and KM4 materials, which are both made of standard polyester, have a slightly lower mass after aging. This phenomenon may be due to the specific properties of the materials and their reaction to aging. Analyzing the graph, after 2500 abrasion cycles, the mass of materials KM1, KM2 and KM4 decreases slightly, while the mass of KM3 increases slightly. This pattern could be related to the material's response to aging, where the structural changes caused by sun exposure may have influenced the mass. After 5000 cycles of abrasion and blowing of the material, a reduction in mass is observed in all samples tested. The percentage of mass reduction is higher in aged samples than in non-aged samples, indicating that aging may accelerate the process of mass loss. In this order, mass decreased by 3.08% for KM1, 2.20% for KM2, 1.61% for KM3 and 2.22% for KM4. This observed difference in percentage mass reduction indicates that aging of the materials can significantly affect their wearability and lead to greater mass loss after a certain number of abrasion cycles. The different results obtained after abrasion of the aged materials, particularly the visible increase in mass in some samples, indicate the possibility of uneven aging of the materials. The more pronounced reduction in mass observed in recycled material (KM1) after 5000 abrasion cycles compared to conventional materials (KM2, KM3, KM4) can be attributed to the unique properties and structural characteristics of recycled polyester.

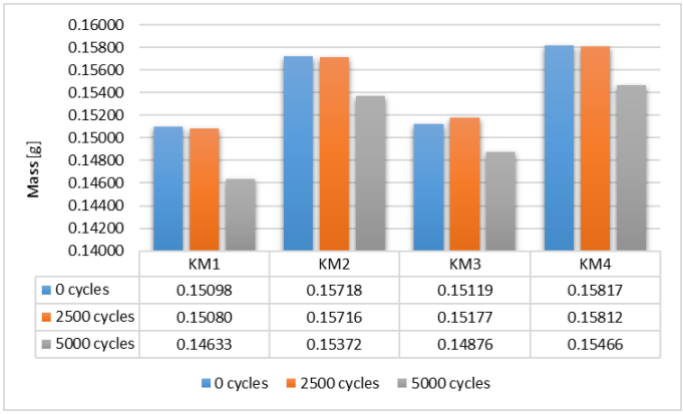

Fig. 3: Graphical presentation of measured masses after a different number of cycles for aged materials

Recycled materials often have different microstructures, potentially making them more susceptible to abrasion. This decrease in mass of recycled polyester can have a significant impact on sports materials. The increased

DOI: https://doi.org/10.26799/cp-tribology-2024

susceptibility to wear and tear can lead to a shorter lifespan of sports materials, which is a crucial factor in material selection in the sports industry.

4. Conclusion

The results of this study show that the abrasion resistance of polyester sportswear materials is influenced by several factors, including the type of polyester and aging. In particular, exposure to sunlight was found to significantly affect the mass and abrasion resistance of the materials. Despite their sustainability benefits, recycled polyester materials exhibited higher susceptibility to abrasion compared to conventional materials. This result underlines the importance of considering both durability and sustainability when selecting materials for sportswear production. Overall, the study provides valuable insights into improving the durability and sustainability of sportswear materials, contributing to improved performance and quality in the sports industry.

Acknowledgements

This work has been fully supported-supported in part by Croatian Science Foundation under the project IP-2020-02-5041 Textile Materials for Enhanced Comfort in Sports - TEMPO.

References

1. I. Salopek Čubrić, G. Čubrić, V. M. Potočić Matković and A. Pavko Čuden, "The comfort of knitted fabric: interaction of sportswear and athlete's body," *Commun. Develop. and Assemb. of Text. Prod.*, vol. 2, no. 1, pp. 70-79, 2021.
2. I. Ziemele, I. Šroma and A. Kakarāne, "Comfort in Sportswear," *Key Eng. Mat.*, vol. 762, pp. 402–407, 2018.
3. B. K. Behera and P. K. Hari, "Friction and other aspects of the surface behavior of woven fabrics," in *Woven Textile Structure*, 2010, pp. 230–242.
4. A. Petrov, I. Salopek Čubrić, G. Čubrić and I. Katić Križmančić, "Assessing the impact of outdoor aging and test settings to abrasion of materials" in Proceedings of the 22th International Conference on Materials, Tribology & Recycling, Zagreb, 2022, pp. 330-344.
5. A. Arora, "Effect of Abrasion Resistance on the Woven Fabric and its Weaves," *Int. J. Sci.: Basic and Appl. Res.*, vol. 50, no. 2, pp. 9-19, 2020.
6. C. Yaping, D.M. Mitrano, R. Hufenus and B. Nowack, "Formation of Fiber Fragments during Abrasion of Polyester Textiles Environmental," *Sci. & Tech.*, vol. 55, no. 12, pp. 8001-8009, 2021.
7. I. Katić Križmančić, I. Salopek Čubrić, V.M. Potočić Matković and G. Čubrić, "Changes in Mechanical Properties of Fabrics Made of Standard and Recycled Polyester Yarns Due to Aging, " *Polymers*, vol. 15, no. 23, pp.1-17, 2023.
8. ISO 12947-3:1998 – Textiles: Determination of the abrasion resistance of fabrics by the Martindale method, Part 3: Determination of mass loss